

AFM Image Analysis Applied To the Investigation of Elementary Reactions in the Synthesis of Comb Star Copolymers

Michel Schappacher and Alain Deffieux*

Laboratoire de Chimie des Polymères Organiques, UMR 5629 CNRS-ENSCP-Université Bordeaux I, 16 Avenue Pey Berland, 33607 Pessac Cedex, France

Received December 2, 2004

Revised Manuscript Received March 18, 2005

The synthesis and study of macromolecular objects of increasing molecular complexity exhibiting specific properties is a very active research domain in close relation with the development of nanosciences and nanotechnologies. To precisely control the chemical composition, dimensions, chain topology, and final properties of these macromolecular entities, synthetic strategies based on the combination of a series of controlled polymerizations, polymer functionalization, and coupling reactions have been developed. Indeed, the successive building steps must be highly selective to reach in a reasonable yield the targeted macromolecular objects. One difficulty is to have adequate characterization techniques to follow the step-by-step assembly of the macromolecules from the first building blocks, which are typical linear homo- or copolymer chains, to the end of the process, corresponding to dense high molar mass macromolecules. Conventional molecular characterization techniques such as spectroscopy (NMR, IR, etc.) and chromatography (SEC, HPLC, etc.) are useful to characterize the molecular structure and dimensions of the first macromolecular building blocks, but become rapidly inappropriate to follow precisely further macromolecule build up. Scattering methods (light, neutron, etc.) allow the determination of the average dimensions and shape of larger macromolecules corresponding to the different stages of the synthesis but do not give any structural insight and are not particularly useful to explain when results deviates from expected. This is typically the problem encountered in the synthesis of hyperbranched polymers with precise chain topologies exemplified by comb-star polymers.¹

The direct visualization of isolated macromolecules by AFM imaging and statistical treatment performed on a large number of molecules was recently used to study the structure of combs, dendrigrafts,² and comb-star polymers^{3–5} and determine the selectivity of various controlled radical polymerization processes. In this paper, a similar strategy is applied to characterize four-arm starlike comb polystyrenes prepared by the combination of living anionic and cationic polymerizations and establish a precise diagnostic of the selectivity of the various elementary reactions used in terms of architecture control and molecular dimensions of the targeted molecules. From this analysis, it is possible to identify the main side reactions occurring during the synthesis, their extent, and impact on the final macromolecules.

The synthesis of four-arm star comb polystyrene was achieved in two stages: (a) synthesis of a four-arm poly-

(styrene-*b*-chloroethyl vinyl ether) backbone¹ and (b) grafting polystyryllithium chains [PSLi] onto the reactive chloroether functions of the poly(chloroethyl vinyl ether) [PCEVE] blocks.^{6,7} The general strategy is summarized in Scheme 1. The four-arm starlike PS₁-*b*-PCEVE backbone was obtained by grafting 4 α -diethoxy acetal polystyryllithium short chains onto pentaerythritol tetrakis(4-chlorobutyl ether) (**I**), used as central connecting point. The four acetal-PS₁ end groups of the corresponding star molecule were then derivatized with trimethylsilyl iodide (TMSI)⁸ and used as a polymerization initiator to start the growth of PCEVE blocks in the presence of CEVE and zinc chloride as catalyst. This yielded a four-arm diblock copolymer in which the polystyryl chains [PS₁] act as a spacer between the central connecting point and the PCEVE branches. As previously described^{1,8} grafting of a new series of polystyryllithium [PS₂Li] chains onto the CEVE units of the PS₁-*b*-PCEVE arms yields the corresponding four-arm star polystyrene comb. The chemistry of the synthesis is summarized in Scheme 2, and experimental details are given as Supporting Information.

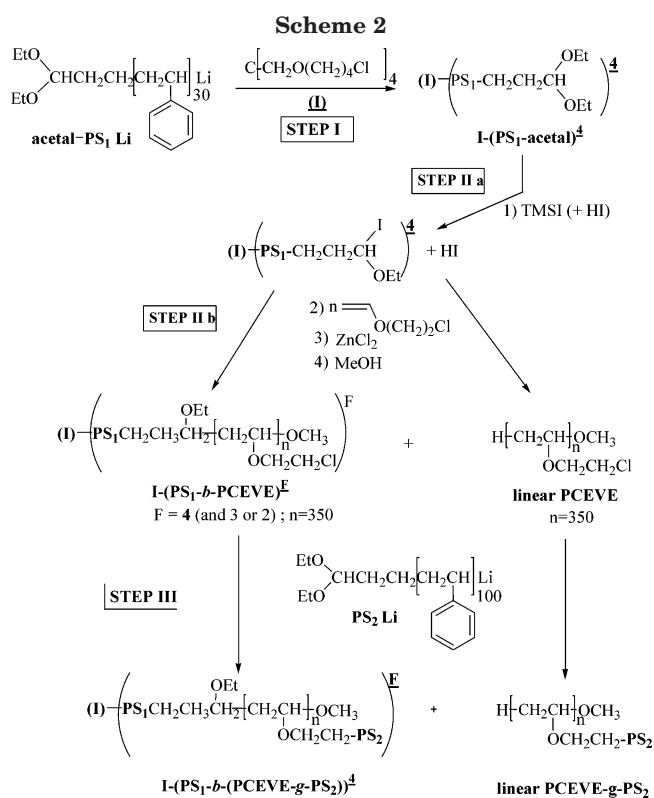
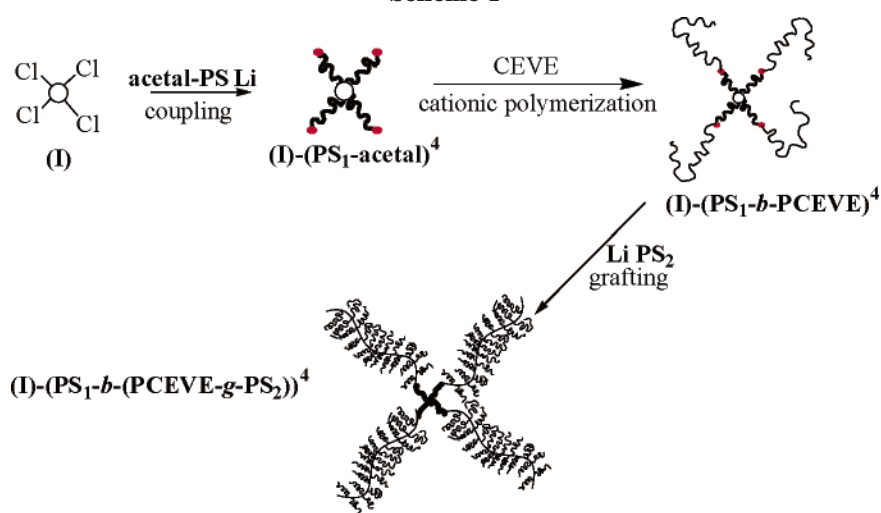
The number of PS₁-acetal arms, F , per precursor molecule, noted as I-(PS₁-acetal),⁴ was determined by ¹H NMR from integrals of characteristics signals of the tetrafunctional organic precursor and the diethylacetal PS block end. F was also calculated from the ratio of the absolute weight molar mass of the I-(PS₁-acetal)⁴ star, determined by dynamic light scattering, to that of the acetal-PS₁ graft corresponding to one arm. Data are collected in Table 1. Both ways yield a number of branches F very close to 4 for I-(PS₁-acetal),⁴ in agreement with a high selectivity of the coupling process.⁶

The corresponding star polystyrene-*b*-PCEVE, noted as I-(PS₁-*b*-PCEVE)⁴ was prepared according to step I. The ratio of the absolute weight molar masses of I-(PS₁-*b*-PCEVE)⁴ to that of the acetal-PS₁ and the homo-PCEVE that constitute together one diblock arm gives an average number of arms, f , of 3.4, see Table 1. The same value is obtained from the empirical relationship¹ between the macromolecule contraction factor g and f ; $g = [(3f - 2)/f^2] = (\bar{M}_{w,app,SEC}/\bar{M}_{w,LS})^{0.43} = 0.86^{0.43}$. These slightly lower experimental f values can be interpreted either by an incomplete initiation of the CEVE polymerization from the four acetal ends of the I-(PS₁-acetal)⁴ precursor and/or by some termination or transfer during the propagation, as will be discussed later in light of the AFM images.

The main characteristics of the “four-arm” comb-star polystyrene I-(PS₁-*b*-(PCEVE- g -PS₂))⁴ are collected in Table 2. Assuming that the contribution of PS₁ molar mass is negligible, the equivalent one-arm linear PCEVE- g -PS₂ comb was prepared separately from a homo-PCEVE and PS₂ grafts. The number of secondary PS₂ branches, F_2 , per comb macromolecule was calculated from the relationship $F_2 = \bar{M}_{w,LS,comb} - \bar{M}_{w,LS,backbone} / \bar{M}_{w,PS_2}$. F_2 values correspond to the substitution of 75–80% of the CEVE units of the PCEVE backbones. As previously discussed, the $\bar{M}_{w,RI(app)}/\bar{M}_{w,LS}$ ratio can be correlated to the volume contraction of the branched molecules with respect to the corresponding linear polymer. It yields molar mass ratios of 0.29 and 0.19, respectively, for the linear and the star combs, in agreement both with the highly branched chain archi-

* Author to whom correspondence should be addressed. E-mail: deffieux@enscp.fr.

Scheme 1



ture of the combs and the much higher volume contraction of the comb star. The corresponding gyration and hydrodynamic radius of the comb polymers are given in Table 2.

Because of their size and high compactness, these highly branched macromolecules can be visualized individually by AFM. Figure 1 shows the topographic and phase images of a series of isolated macromolecules, which confirms the predominant formation of the four-arm comb stars. Interestingly, we can observe, on an isolated four-arm molecule, Figure 2, the lower core section of the comb star corresponding to the connected 4 central PS₁ block spacers, likely in extension. The selectivity of the synthetic pathway was examined in more detail through direct analysis of a set of individual macromolecules (300) prepared according to Scheme 1. In this study, each star polymer was individually characterized by counting their number of arms and measuring their length. Although the proportion of four-

arm comb stars, Figure 1, largely predominates, analysis of the image indicates the presence of stars with a lower number of arms. The presence of three-arm stars and of a very small amount of two-arm stars (long linear combs), Figure 3b, is observed. The formation of these structures can be attributed to incomplete initiation of CEVE polymerization from the acetal termini of the I-(PS₁-acetal)⁴ precursor. Moreover, among the four- and three-arm star macromolecules, we can also distinguish between symmetric stars constituted of four or three arms of relatively close length and asymmetric stars, which possess one or even two much shorter arms, Figures 3c and 1c, typically less than 1/2 of the average arm length. The different structures identified and their percentages are indicated in Table 3.

It can be assumed that the PS₂ grafting reaction on the CEVE units is a random and homogeneous process that does not modify the primary structure of the backbone macromolecule, i.e., the number of arms and the relative initial branch dimensions (DP_n). We may thus consider that analysis of AFM images can give an insight into the elementary chemical processes involved in the building of the star polymer. As already discussed, the relative amounts of four-, three-, and two-arm star fractions (symmetric + asymmetric) can be used to quantify the efficiency of the initiation step of the CEVE polymerization from the acetal-PS₁ ends, step II of Scheme 2. This yields an initiation efficiency of 91% with respect to the acetal functions, see Table 4. Besides, the presence of stars with much shorter arms observed by AFM can be attributed to the aborted growth of some PCEVE branches during the CEVE propagation step. This is indicative of the presence of some transfer and/or termination reactions during the CEVE propagation reaction, step IIb of Scheme 2. This implies that, in addition to side initiation by hydrolyzed TMSI, a fraction of the linear PCEVE chains could result from such side reactions.

The impact of these two side processes is a reduction of the efficiency in the building of stars with a controlled number of arms, Table 4. It corresponds to the formation of stars with a lower average number of arms than targeted, presently 3.25, a value in very good agreement with the numbers given in Tables 1 and 2.

In conclusion AFM image analysis of isolated high molar mass hyper-branched macromolecules is not only a powerful tool to investigate their size and architecture

Table 1. Dimensions and Characteristic Parameters of Four-arm Comb Precursors and of the Corresponding Linear Building Blocks

ref	\bar{M}_{nSEC} apparent	\bar{M}_{wSEC} apparent	I_p	\bar{M}_{wLS}	F	$\bar{M}_{wapp}/\bar{M}_{wstar}$	f
linear PS ₁ -acetal ^a	2800	3040	1.08	-	-	-	-
I-(PS ₁ -acetal) ^{4b}	9000	9600	1.06	11800	3.9 ^d	-	-
linear PCEVE ^c	42000	44000	1.06	35400	-	-	-
I-(PS ₁ - <i>b</i> -PCEVE) ^{4c}	96600	114000	1.18	132000	3.4 ^e	0.86	3.4 ^f

^a Sampled from acetal-PS₁Li solution before grafting. ^b After elimination of residual ungrafted acetal-PS₁. ^c Recovered after fractionation of the crude I-(PS₁-*b*-(PCEVE-))⁴ solution. ^d Determined both by NMR and from the ratio \bar{M}_{wLS} I-(PS₁-acetal)⁴/ \bar{M}_{wSEC} linear PS₁. ^e Determined from the ratio \bar{M}_{wLS} I-(PS₁-*b*-PCEVE)⁴/ $(\bar{M}_{wSEC}$ linear PS₁-acetal + \bar{M}_{wSEC} linear PCEVE). ^f Determined from the relationship¹ $g = (\bar{M}_{wappSEC}/\bar{M}_{wLS})^{0.43} = [(3f - 2)/f^2]$.

Table 2. Main Characteristics of the Linear and Corresponding Four-Arm Star PS Combs

ref	$10^6 \bar{M}_w$ th g/mole	$10^6 \bar{M}_w$ SEC (app) g/mole	I_p	$10^6 \bar{M}_w$ LS g/mole	F	grafting %	$\bar{M}_{napp}/\bar{M}_{nstar}$	Rg^b nm	Rh^b nm
linPCEVE- <i>g</i> -PS ₂	3.4	0.8	1.09	2.7	-	79	0.29	25	24
I-(PS ₁ - <i>b</i> -(PCEVE- <i>g</i> -PS ₂) ^a) ⁴	11.8	1.7	1.07	9.0	3.34	76	0.19	45	45

^a PS₂ graft: \bar{M}_{wSEC} , 10400 g/mole; $I_p = 1.03$. ^b Determined in THF at 25 °C.

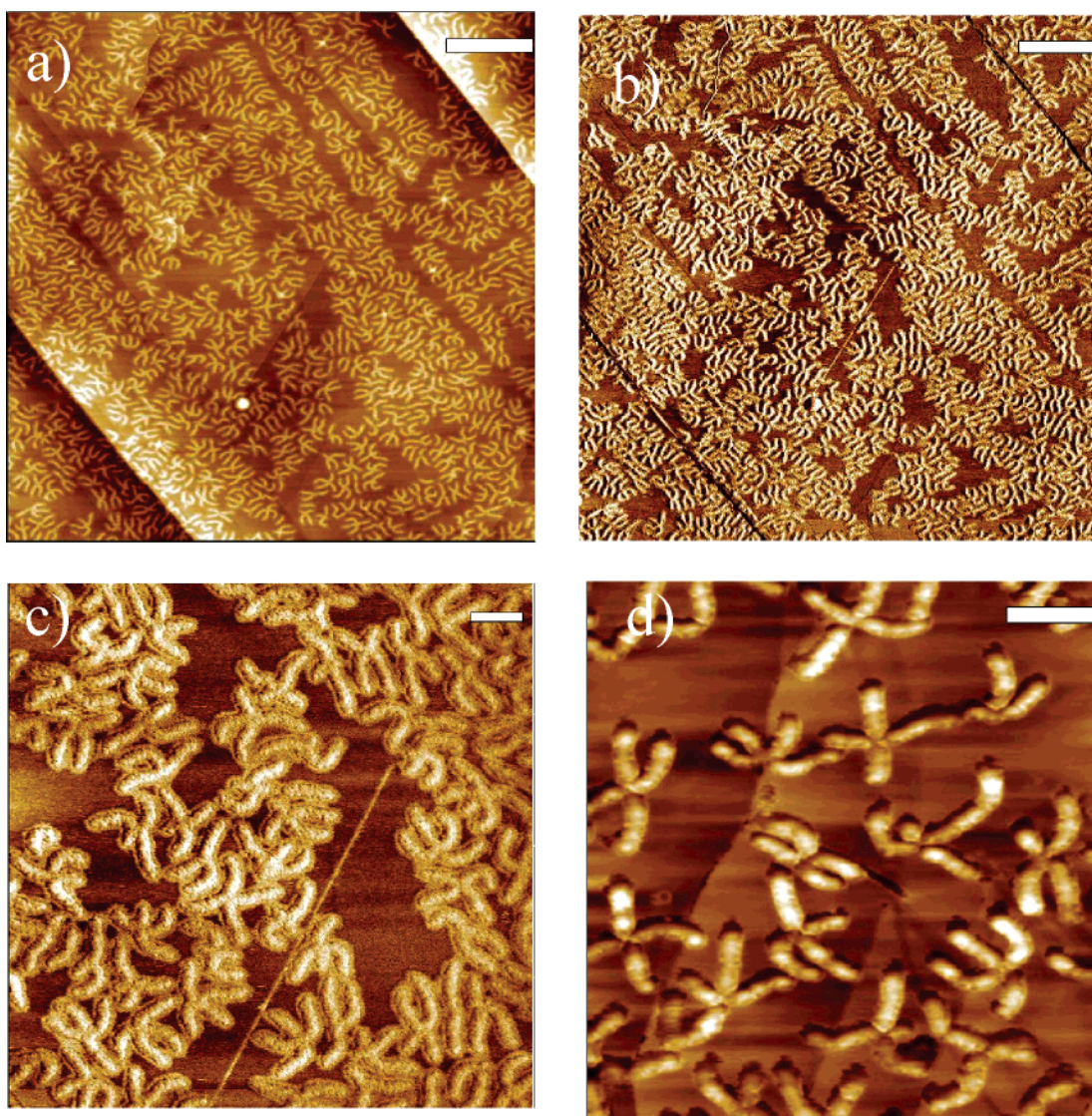


Figure 1. AFM images of the tetra-arm comb stars I-(PS₁-*b*-PCEVE-*g*-PS₂)⁴ obtained from HOPG deposits of their CH₂Cl₂ solution. (a, b) Large-scale phase and topographical images: bar = 300 nm; (c, d) Zoomed phase and topographical images: bar = 100 nm.

but it allows the examination in detail of some of the elementary chemical processes involved in their construction and may highlight the side reactions occurring during their synthesis.

In the present study, AFM images point out that, during the synthesis of 4-branch star backbone by “controlled” cationic polymerization, the initiation of CEVE polymerization from acetal groups of the core

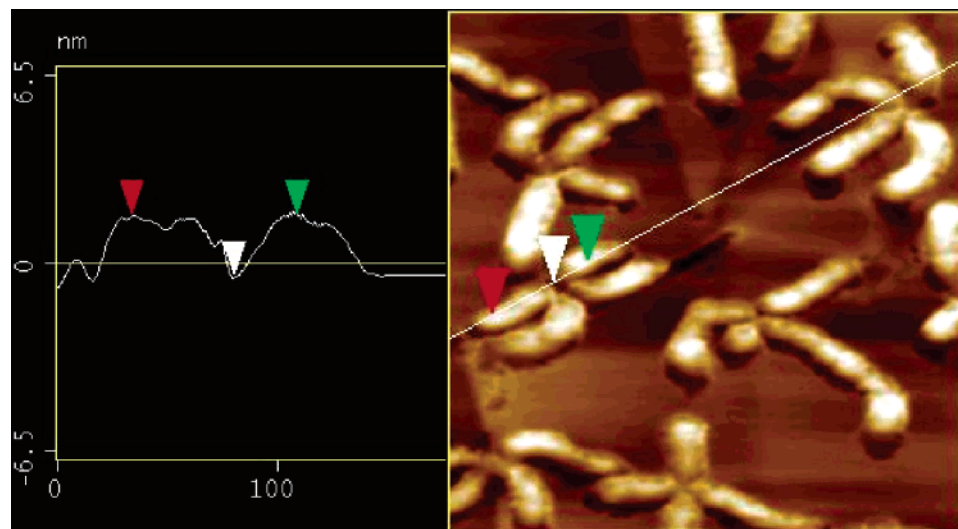


Figure 2. AFM image of isolated tetra-arm comb stars (I)-(PS₁-*b*-PCEVE-*g*-PS₂)⁴ showing the cross section across two arms of a comb star molecule.

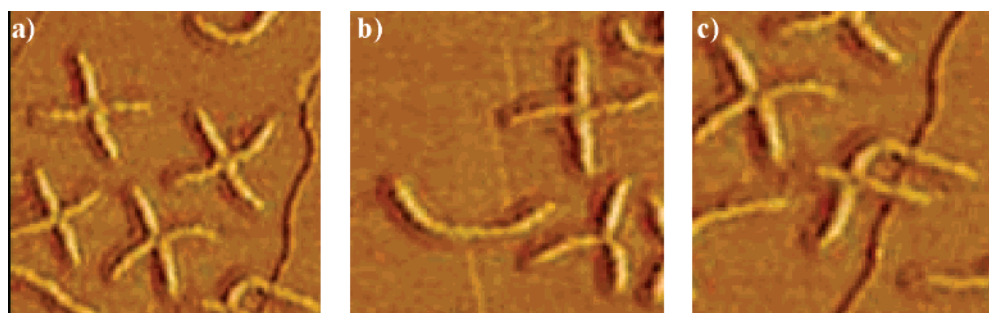


Figure 3. AFM images of isolated tetra-arm comb stars (I)-(PS₁-*b*-PCEVE-*g*-PS₂)⁴ showing regular four-arm comb (a) and stars exhibiting structural defects, (b) three- and two-arm comb stars, and (c) four-arm comb star with an aborted arm.

Table 3. Structures and Percentages of the Different Comb Stars as Determined by AFM Analysis^a

% 4-arm star			% 3-arm star		% linear (2 and 1 arms)	
76			21		3	
sym.	assym.		sym.	assym.	-	
% 4 arms ^b	% 3 + 1 degen ^c	% 2 + 2 degen ^c	% 3 arms ^b	% 2 + 1 degen ^c	% equal to 2 arms ^b	% 1 arm
47	25	4	19	2	3	≪1

^a Each polymer molecule was individually characterized by counting its number of arms (ranging from 4 to 1) and measuring the length of each arm. ^b All the arms have about the same length. ^c One arm (or two) has a length that is less than 1/2 of the average arm length, and it is counted as degenerated (degen).

Table 4. Analysis of Elementary Reaction Processes through Statistical Investigation of AFM Images of Isolated Four-arm Polystyrene Comb Stars

Efficiency of CEVE initiation from PS ₁ acetal-ends ^a %	% of size-controlled PCEVE arms ^b	Overall arm efficiency ^c %	Average number of controlled arms F ^r per star molecule ^d
91	91	81	3.25

^a $I_{\text{eff}} = 4(\% \text{ 4-arm star}) + 3(\% \text{ 3-arm star}) + 2(\% \text{ 2-arm star})/4 \times 100$. ^b $\%(\text{number of sized-controlled arms}/\text{total number of arms})$: $4(\% \text{ 4 arms}) + 3(\% \text{ (3 + 1) arms}) + 2(\% \text{ (2 + 2) arms}) + 3(\% \text{ (3 arms)}) + 2(\% \text{ (2 + 1) arms}) + 2(\% \text{ 2 arms})/(\% \text{ 4 arms} + \% \text{ 3 arms} + \% \text{ 2 arms})$. ^c $\% \text{ Initiation eff} \times \% \text{ size-controlled arms}$. ^d $F^r = 81 \times 4/100$.

precursor is not quantitative and that some transfer or termination also takes place during the propagation reaction. As shown by AFM, although the contribution of each of these two side processes is relatively small (less than 10% contribution for each), they already significantly affect the purity of the targeted four-arm star comb polymers.

Supporting Information Available: Experimental procedures. This material is available free of charge via the Internet at <http://pubs.acs.org>.

References and Notes

- Deffieux, A.; Schappacher, M. *Macromolecules* **2000**, *33*, 7371.
- Viville, P.; Leclère, P.; Deffieux, A.; Schappacher, M.; Bernard, J.; Borsali, R.; Brédas, J. L.; Lazzaroni, R. *Polymer* **2004**, *45*, 1833.
- Matyjaszewski, K.; Qin, S.; Boyce, J. R.; Shirvayants, D.; Sheiko, S. S. *Macromolecules* **2003**, *36*, 1843.
- Boyce, J. R.; Shirvayants, D.; Sheiko, S. S.; Ivanov, A., D.; Börner, H.; Qin, S.; Matyjaszewski, K. *Langmuir* **2004**, *20*, 6005.

- (5) Sheiko, S. S.; Da Silva, M.; Shirvayants, D.; LaRue, I.; Prokhorova, S.; Moeller, M.; Beers, K.; Matyjaszewski, K. *J. Am. Chem. Soc.* **2003**, *125*, 6725.
- (6) Deffieux, A.; Schappacher, M. *Macromolecules* **1999**, *32*, 1797.
- (7) Schappacher, M.; Deffieux, A. *Makromol. Chem. Phys.* **1997**, *198*, 3953.
- (8) Schappacher, M.; Deffieux, A. *Macromolecules* **2001**, *34*, 7595.

MA047518Y